

# WW Horologii: X-ray and optical observations

Allyn F. Tennant,<sup>1</sup> Jeremy Bailey,<sup>2</sup> D. T. Wickramasinghe,<sup>3</sup> Kinwah Wu,<sup>4</sup>  
Lilia Ferrario<sup>3</sup> and J. Hough<sup>5</sup>

<sup>1</sup>ES-65, Space Science Laboratory, NASA Marshall Space Flight Center, Huntsville, AL 35812, USA

<sup>2</sup>Anglo–Australian Observatory, Epping, NSW 2121, Australia

<sup>3</sup>Department of Mathematics, The Australian National University, Canberra, ACT 0200, Australia

<sup>4</sup>Research Centre for Theoretical Astrophysics, School of Physics, The University of Sydney, NSW 2006, Australia

<sup>5</sup>Department of Physical Sciences, University of Hertfordshire, Hatfield, Hertfordshire AL10 9AB

Accepted 1994 August 22. Received 1993 December 21; in original form 1993 August 4

## ABSTRACT

The eclipsing AM Herculis binary WW Hor (EXO 023432–5232.3) was observed in the X-ray band with the *ROSAT* satellite and in the optical band with the 3.9-m telescope of the Anglo–Australian Observatory. A clear eclipse is seen in the X-ray light curve of this system for the first time. The relative location of the X-ray eclipse suggests that the accretion pole on the white dwarf surface has migrated in the last few years, consistent with the optical data. The 0.2–2 keV spectrum is well fitted with an absorbed power-law model. There is no indication of a soft blackbody component, although such a component could be masked by the absorption. The X-ray luminosity of the system in the 0.2–2 keV band is  $1.0 \times 10^{31}$  erg s<sup>-1</sup>.

**Key words:** binaries: close – stars: individual: WW Hor – stars: magnetic fields – novae, cataclysmic variables – X-rays: stars.

## 1 INTRODUCTION

The eclipsing AM Herculis binary WW Hor (EXO 023432.5) was discovered as a serendipitous X-ray source (Beuermann et al. 1987) and was observed twice, during 1983 September and 1984 December, by *EXOSAT*. The orbital period of the system is 115.5 min (Beuermann et al. 1990), and the distance is 430 pc (Bailey et al. 1988). The instruments on *EXOSAT* did not have a high enough sensitivity to obtain a good quality light curve and spectrum of the system. The eclipse which can be seen in the optical bands (Bailey et al. 1988) therefore cannot be resolved in the X-ray light curves. Neither has the X-ray luminosity, nor the location, nor the size nor the effective temperature of the X-ray emission region been determined. Optical observations of WW Hor (Bailey et al. 1988; Beuermann et al. 1990) were performed 30 months after the *EXOSAT* observations. During the time lapse between the optical and X-ray observations, WW Hor might have changed its accretion state many times, as AM Hers generally can alternate between high and low accretion states within months. This makes the comparison between the optical and X-ray observations difficult.

In 1991 November and December and 1992 July, we observed WW Hor in the X-ray band using the *ROSAT* satellite. On 1992 July 29, a follow-up optical observation was carried out using the 3.9-m telescope of the Anglo–

Australian Observatory (see Bailey et al. 1993). Since the time lapse between the X-ray and the optical observations in 1992 was relatively short, it is reasonable to assume that the accretion state of the system had not changed significantly (although AM Hers can change their accretion states within days). By comparing the X-ray and optical data, we are able to determine the properties of the shock-heated emission region of the system.

## 2 OBSERVATIONS

WW Hor was observed using the PSPC2 instrument (Pfeffermann et al. 1986) on board the *ROSAT* satellite on 1992 July 21, 22 and 23. The total on-target time of the 1992 observation was 15 300 s. We noticed that the active galaxy ESO 198–G24 also lies in the *ROSAT* field of view and was observed by J. Turner on 1991 November 28, and December 21 and 22. We therefore obtained an additional 5090-s observation of the system from Turner's data. The 1991 observation does include an eclipse, which is seen, and also confirms the basic conclusions of the 1992 observation. Unfortunately, the separation of the two sources was such that, when ESO 198–G24 was centred, WW Hor lay near one of the supporting ribs in the detector. For this reason, all the results in this paper are based on the analysis of the 1992 observation, in which WW Hor is at the centre of the field.

The good time intervals of the observations are listed in Table 1. The follow-up optical observation was performed on 1992 July 29 with the 3.9-m telescope of the Anglo-Australian Observatory. The optical brightness of WW Hor was  $\approx 20$  mag during the observation, indicating that the system was in a low accretion state. Light curves in the red (5500–8400 Å) and blue (3400–5300 Å) bands were obtained.

### 3 RESULTS AND DISCUSSIONS

We fold the data using the eclipse ephemeris

$$T_0 = \text{HJD } 244\,7126.127\,82 + 0.080\,199\,035$$

given in Beuermann et al. (1990). The X-ray light curves of the 1992 observation are shown in Fig. 1. The upper panel corresponds to the energy channels 1–40 (0.1–0.5 keV); the lower panel corresponds to the energy channels 41–240 (0.5–2.0 keV). The two light curves have very similar shapes. In both energy bands, the count rate rises sharply at phase 0.75 and declines sharply at phase 1.25. The bright phases occupy about one-half of the total orbital period. The maximum fluxes at the bright phases for the high- and low-energy channels are 0.06 and 0.04 count  $\text{s}^{-1}$ , respectively. The flux for channels 1–40 is about 0.01 count  $\text{s}^{-1}$ , and the flux for channels 41–240 is consistent with zero, during the faint phases.

An eclipse can be seen clearly at phase 1.0, and it is also present in the light curve of the 1991 observation (not shown). However, the eclipse was not revealed in the previous *EXOSAT* observations because of the quality of the data. The centre of the eclipse is almost at the orbital phase 1.0 (0.0), in agreement with the optical observations by Bailey et al. (1988) and Beuermann et al. (1990). When we use a Gaussian to fit the bright-phase intensity and a negative

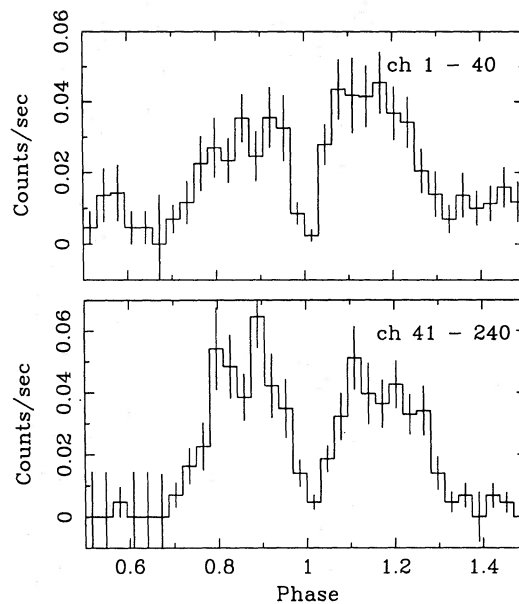


**Figure 1.** The X-ray light curves of WW Hor. The upper and lower panels correspond to the energy channels 1–40 (0.1–0.5 keV) and 41–240 (0.5–2.0 keV), respectively. The data are folded using the eclipse ephemeris  $T_0 = \text{HJD } 244\,7126.127\,82 + 0.080\,199\,035$  given in Beuermann et al. (1990).

**Table 1.** X-ray observations.

Date	start	end	accepted time
28 Nov 1991	12:53:53	13:00:33	0400 s
21 Dec 1991	09:58:22	10:18:07	1185 s
21 Dec 1991	11:35:23	11:53:57	1110 s
21 Dec 1991	19:34:53	19:52:56	1083 s
22 Dec 1991	08:17:23	08:39:17	1314 s
21 July 1992	10:55:45	11:06:53	0668 s
21 July 1992	15:41:37	16:10:41	1742 s
21 July 1992	17:17:23	17:48:25	1862 s
21 July 1992	18:52:47	19:24:11	1884 s
22 July 1992	17:12:17	17:42:55	1836 s
22 July 1992	18:46:37	19:18:25	1908 s
23 July 1992	15:29:20	16:01:10	1910 s
23 July 1992	17:05:27	17:37:10	1903 s
23 July 1992	18:46:16	19:12:56	1600 s

Gaussian to fit the eclipse, we find that the centres of the Gaussians are at phase 1.022 and phase 1.012, respectively. The difference in the centres of the Gaussians suggests that the X-ray emission region is trailing the secondary star, with a phase lag of roughly  $4^\circ \pm 3^\circ$ . This value is consistent with that deduced from our optical data (see Bailey et al. 1993). Previous observations of WW Hor by Bailey et al. (1988), however, showed that its emission region led the secondary star by a phase of  $11^\circ \pm 2^\circ$ . Thus the accretion pole of WW Hor has migrated in the past few years. A similar phenomenon was also observed in another eclipsing AM Her system, DP Leo (Bailey et al. 1993). As the accretion pole migration in these systems has been reported separately in Bailey et al. (1993), we will not discuss it in detail here. For theoretical explanations of this phenomenon, see Wickramasinghe & Wu (1991), Wu & Wickramasinghe (1993), Bailey et al. (1993), and references therein.

In Fig. 2, we show the red-band (5500–8400 Å) and the blue-band (3400–5300 Å) light curves of the optical observations. The flux calibration of the data is given based on the observations of standards from Graham (1982). The eclipse is also clearly seen in the two light curves. The red light curve has a sharp rise in the intensity at the beginning of the bright phases and a rapid decline at the end of the bright phases. The general structures of the red light curve and the X-ray light curves are not similar. The strong phase dependence of the intensity variations in the red band can be explained easily by the beaming of cyclotron emission from a shock-heated region (e.g. Chanmugam & Dulk 1981; Meggitt & Wickramasinghe 1982). The blue light curve is, however, very different – the intensity rises gradually at the beginning of the bright phase and declines gradually at the end, with the maximum occurring near the centre of the bright phase. Such intensity variations are atypical of cyclotron emission, even

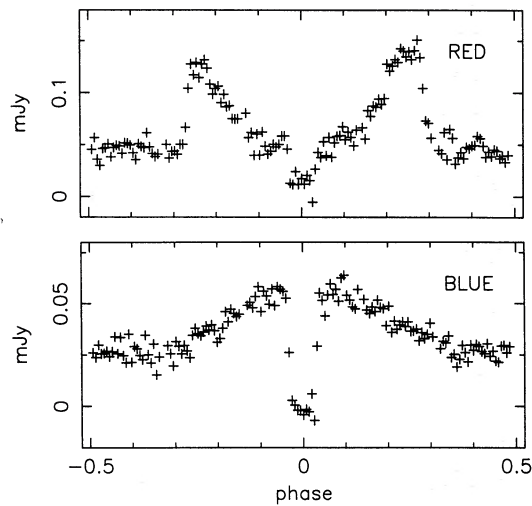


**Figure 2.** The red- (5500–8400 Å) and blue- (3400–5300 Å) band light curves of WW Hor. The data are folded on the orbital period (see Bailey et al. 1993 for details).

when inhomogeneities in the emission region are taken into account (see Wu & Wickramasinghe 1991). The observed variations are, however, typical of what is expected for emission from an optically thick region close to or on the white dwarf surface, and can be explained as a combination of limb darkening and changes in the effective projected area of the emission region. We note that a similar blue light curve was also observed for V834 Cen during its low accretion state (Ferrario et al. 1992) and was attributed to blackbody radiation from the heated white dwarf surface.

The PSPC2 instrument on board *ROSAT* provides spectral information on the X-ray photons. We use only the 1992 observation to construct the X-ray spectrum. We model the spectrum by folding a test spectrum through the response matrix for the detector and comparing the result with the data. We find an acceptable fit to either an absorbed power-law or an absorbed thermal bremsstrahlung spectrum. For the fit to the power-law case, the power-law function has an index  $1.97 \pm 0.36$  (90 per cent confidence, single parameter uncertainty) with some low-energy absorption of  $1.80 \pm 0.84 \times 10^{20} \text{ atom cm}^{-2}$  (Fig. 3). We also find that an absorbed thermal bremsstrahlung model with  $kT = 1.5^{+1.8}_{-0.5}$  keV can fit the spectrum. This temperature is less than the typical bremsstrahlung temperature ( $\sim 10$  keV) of AM Hers in high accretion states (see Beuermann 1988). The observed X-ray flux is  $3.6 \times 10^{-13} \text{ erg cm}^{-2} \text{ s}^{-1}$  in the 0.2 to 2.0 keV band, and the unabsorbed X-ray flux is about  $4.4 \times 10^{-13} \text{ erg cm}^{-2} \text{ s}^{-1}$ . For a distance of 430 pc (Bailey et al. 1988), the corresponding X-ray luminosity in this energy band is  $\sim 1.0 \times 10^{31} \text{ erg s}^{-1}$ . If we take two as the value of the power-law index and assume that the power-law continues to 20 keV, the luminosity in the 2.0–20 keV band is then approximately equal to the luminosity in the 0.2–2.0 keV band. Thus the total luminosity in the 0.2–20 keV band is  $\sim 2 \times 10^{31} \text{ erg s}^{-1}$ . This value is near the low end of the typical hard X-ray luminosity of the AM Her binaries and is consistent with luminosities of these systems in their low accretion state.

Generally, the X-ray spectrum of AM Hers consists of a power-law hard X-ray component and a blackbody soft

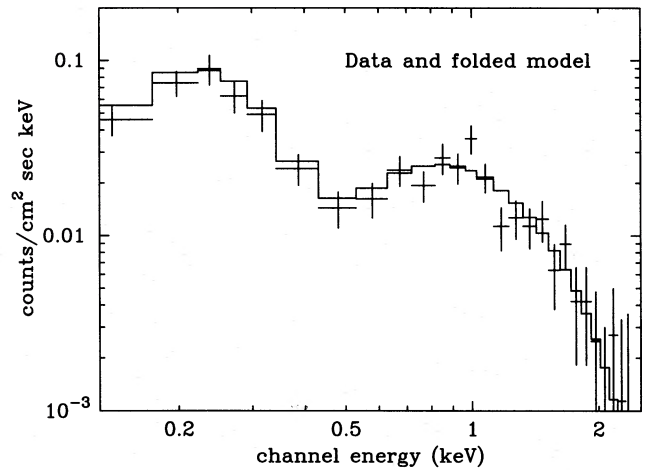


**Figure 3.** The model power-law X-ray spectrum of WW Hor. The power-law index of the spectrum is  $1.97 \pm 0.36$  (90 per cent confidence, single parameter uncertainty) and the column density of the low-energy absorption is  $1.80 \pm 0.84 \times 10^{20} \text{ atom cm}^{-2}$ .

X-ray component (Rothschild et al. 1981; Beuermann 1988). The power-law component is probably the sum spectrum of optically thin bremsstrahlung radiation emitted from shock-heated regions with different temperatures. The blackbody component may be due to the reprocessing of the hard X-rays (Beuermann 1988; Stockman 1988) and/or other mechanisms such as thermal emission due to blobby accretion (Hameury & King 1988; Litchfield 1990). Therefore it is also necessary to consider the implication of an additional blackbody component. Unfortunately, the X-ray flux of WW Hor was weak, partly because it was in a low accretion-rate state and partly because its distance is large. Furthermore, the interstellar absorption in the soft X-ray band is very strong, and an upturn in the soft X-ray band can be countered by increasing the interstellar absorption. If we use only the X-ray data, we are unable to constrain the blackbody component. As WW Hor was in a very low accretion state during the 1992 observation, we speculate that the total accretion luminosity of the system might not be strong enough to power a strong UV and soft X-ray blackbody reprocessed component as is found in typical AM Hers in a high accretion state. Rather, the peak of the blackbody reprocessed component in WW Hor was probably shifted to a lower frequency, and the blue light may be dominated by the low-energy tail of the blackbody component, and the emission from the white dwarf itself. Unfortunately, due to the faintness of the system, we did not obtain reliable polarimetric data, which would have enabled us to confirm the non-cyclotron origin of the blue light. However, as we have already noted, the blue light in the optical band can be related to an optically thick blackbody component. In an attempt to constrain the blackbody component, we postulate that the excess blue light in the bright phase is due to the low-energy tail of the blackbody component. Thus the blue-band flux will constrain the Rayleigh–Jeans part of the blackbody component and the X-ray data will constrain the Wien part.

To estimate the contribution of the blackbody X-ray component to the blue-band flux we consider the following. We assume the blue flux during the X-ray-faint phases is due to

the thermal emission from the white dwarf and the excess blue flux at the X-ray-bright phases is the contribution of the soft tail of the blackbody X-ray component. We note that the difference between the blue fluxes at the X-ray-faint phases and the centre of the eclipse is about 0.025 mJy, which corresponds to a luminosity of a white dwarf with a radius of  $10^9$  cm and a surface temperature of  $\sim 10^5$  K. Therefore our assumption is consistent with the typical white dwarf parameters of the AMHers. From the maximum of the light curve, we estimate the phase-average blue-band flux to be roughly 0.02 mJy, without correction for reddening effects. (Clearly, the blue flux would be increased if corrected for reddening.) We then consider a two-component model consisting of a power-law and a blackbody component and fit both the blue-band flux and the *ROSAT* spectrum simultaneously, using the *XSPEC* spectral fitting program (Shafer et al. 1991). An *XSPEC* response matrix is constructed for the blue band using the data from Allen (1973). We further assume that the power-law component is cut off below the soft X-ray band and therefore there is no power-law contribution to the blue-band flux. For this model, the blue-band flux effectively constrains the normalization of the blackbody, and the lack of an upturn in the X-ray effectively sets an upper limit on the temperature. We do not constrain the absorption, and so *XSPEC* allows both the temperature and absorption to be high, provided that this generates a model that is consistent with the data in a statistical sense. Fitting this two-component model, we find that the luminosity of the power-law component in the 0.2–2.0 keV band is  $8 \times 10^{30}$  erg s $^{-1}$  and the spectral index is  $2.0 \pm 0.4$ . The blackbody component has a temperature of  $19^{+3}_{-2}$  eV. The absorption corresponds to  $8 \pm 3 \times 10^{20}$  atom cm $^{-2}$ . The 90 per cent confidence *upper limit* of the blackbody luminosity is  $1.1 \times 10^{34}$  erg s $^{-1}$ , corresponding to an area of the emission region of  $< 8 \times 10^{16}$  cm $^2$ . We note that there is a viewing angle  $\theta$  between the line of sight and the normal of the emission region. A factor of  $1/\cos \theta$  should therefore be included in the inferred upper limit of the area of the emission region. Also, the maximum luminosity obtained is the maximum luminosity that is consistent with the observed blue and X-ray fluxes. If the absorption is lower, a smaller total luminosity consistent with our data could be obtained. When the temperature takes the value of the upper limit, the absorption and blackbody cancel each other, such that the model spectrum appears to continue the power law to lower energies. Since it is rather unlikely for this precise cancellation to occur, the true blackbody temperature is expected to be much lower than the upper limit, and hence the luminosity is also lower. However, the current data cannot resolve this issue.

## 5 CONCLUSIONS

WW Hor was observed in the X-ray band using the *ROSAT* satellite and in the optical band using the Anglo-Australian Telescope. The system was in a low accretion state during the

1992 observation, inferred from its optical brightness. The eclipse is seen for the first time in the X-ray band. The centre of the X-ray eclipse is at phase 0.0 (1.0), which is in agreement with that of the optical observations. From the location of the eclipse in the light curve, we find that the emission region trailed the companion star by  $4^\circ \pm 3^\circ$  during the 1992 observation. The X-ray spectrum at 0.2–2.0 keV has a power-law shape, and the value for the power-law index is  $1.97 \pm 0.36$ . The X-ray spectrum can also be fitted by a thermal bremsstrahlung spectrum with  $kT = 1.5^{+1.8}_{-0.5}$  keV. The X-ray luminosity of the system is  $\sim 1.0 \times 10^{31}$  erg s $^{-1}$  in the 0.2–2.0 keV band. There is no clear indication of a soft blackbody component. However, if we assume that the excess flux in the blue band during the X-ray-bright phases is due to the presence of a soft blackbody component, we obtain an upper limit of  $1.1 \times 10^{34}$  erg s $^{-1}$  for the blackbody luminosity.

## ACKNOWLEDGMENTS

We thank Jane Turner for providing the data of the 1991 *ROSAT* observations and the referee for valuable comments.

## REFERENCES

- Allen C. W., 1973, *Astrophysical Quantities*. The Athlone Press, London, Chap. 10
- Bailey J., Wickramasinghe D. T., Hough J. H., Cropper M., 1988, *MNRAS*, 234, 19P
- Bailey J., Wickramasinghe D. T., Ferrario F., Hough J. H., Cropper M., 1993, *MNRAS*, 261, L31
- Beuermann K., 1988, in Coyne G. V., Moffat A. F. J., Tapia S., Magalhães A. M., Schulte-Ladbeck R. E., Wickramasinghe D. T., eds, *Polarized Radiation of Circumstellar Origin*. Vatican Obs., Vatican City, p. 125
- Beuermann K., Thomas H. C., Giommi P., Tagliaferri G., 1987, *A&A*, 175, L9
- Beuermann K., Thomas H. C., Schwöpe A. D., Giommi P., Tagliaferri G., 1990, *A&A*, 238, 187
- Chanmugam G., Dulk G. A., 1981, *ApJ*, 244, 569
- Cropper M., 1990, *Space Sci. Rev.*, 54, 195
- Ferrario L., Wickramasinghe D. T., Bailey J., Hough J. H., Tuohy I. R., 1992, *MNRAS*, 256, 252
- Graham J. A., 1982, *PASP*, 94, 244
- Hameury J. M., King A. R., 1988, *MNRAS*, 235, 433
- Litchfield S. J., 1990, in Mauche C. W., ed., *Accretion-Powered Compact Binaries*. Cambridge Univ. Press, Cambridge, p. 339
- Meggitt S. M. A., Wickramasinghe D. T., 1982, *MNRAS*, 198, 71
- Pfeffermann E. et al., 1986, *Proc. SPIE*, 733, 519
- Rothschild R. E. et al., 1981, *ApJ*, 250, 723
- Shafer R. A., Haberl F., Arnaud K. A., Tennant A. F., 1991, *XSPEC User's Guide*. ESA TM-09, ESA, Paris
- Stockman H. S., 1988, in Coyne G. V., Moffat A. F. J., Tapia S., Magalhães A. M., Schulte-Ladbeck R. E., Wickramasinghe D. T., eds, *Polarized Radiation of Circumstellar Origin*. Vatican Obs., Vatican City, p. 237
- Wickramasinghe D. T., Wu K., 1991, *MNRAS*, 253, 11P
- Wu K., Wickramasinghe D. T., 1991, *MNRAS*, 246, 686
- Wu K., Wickramasinghe D. T., 1993, *MNRAS*, 260, 141